

Asymmetric bubble disconnection: persistent vibration evolves into smooth contact

Konstantin S. Turitsyn*, Lipeng Lai, and Wendy W. Zhang

Physics Department and the James Franck Institute University of Chicago, Chicago IL 60637

**Also at Landau Institute for Theoretical Physics, Moscow Russia*

(Dated: June 18, 2022)

Focusing a finite amount of energy dynamically into a vanishingly small amount of material requires that the initial condition be perfectly symmetric. In reality, imperfections are always present and cut-off the approach towards the focusing singularity. The disconnection of an underwater bubble provides a simple example of this process. An initial asymmetry in the shape of the bubble neck excites vibrations that persist over time. Often the vibrations evolve into a smooth contact that severs the neck into several lobes.

PACS numbers: 47.20.Ma, 47.55.df, 47.15.km

Whenever a diver plunges into a swimming pool or a waterfall hits a river, air is entrapped by the impact, often as large cavities that subsequently break-up into many pieces [1]. Bubble disconnection is a simpler version of the same collapse dynamics. The most efficient way to divide a submerged air bubble into several bubbles is an axisymmetric implosion. The neck of the air bubble contracts inwards and finally breaks at a single point. In the continuum model [2, 3, 4, 5, 6, 7, 8], the axisymmetric dynamics results in the formation of a focusing singularity in the exterior flow [9]. As water outside the bubble neck rushes inwards to constrict the neck of air, the motion converts the potential energy available at the beginning of the disconnection into kinetic energy. Since the amount of water rushing inwards decreases to 0 as the neck radius goes to 0, all the kinetic energy is condensed into a vanishingly small amount of material at break-up.

Nearly all the previous studies analyzed the implosion by assuming that the axisymmetric implosion prevails. However, new studies [9, 10] reveal that the effect of an initial asymmetry becomes important in the final moments of disconnection. As an example, consider Fig. 1. A slight azimuthal asymmetry is imposed onto the initial shape of the bubble neck by quasi-statically releasing the bubble from a slightly-tilted nozzle. Near the disconnection, the bubble neck evolves into two side-by-side vertical lobes, which subsequently break-up and form two side-by-side satellite bubbles, qualitatively different from the implosion into a point predicted by the axisymmetric model. Recently, Schmidt et al. [9] used experiments and linear stability analysis to show that the memory of the initial asymmetry is encoded by vibrations in the cross-section shape of the bubble neck. These vibrations persist over time with the same amplitudes, thus encoding a detailed memory of the initial distortion. Such a detailed memory is surprising and important because the severely nonlinear evolution towards a singularity is commonly thought to be governed by convergence onto a universal dynamics, one independent of initial conditions and thus possessing little memory of the initial state [11, 12, 13].

Here we focus on consequences of memory which cannot be addressed within the assumption of weak distor-

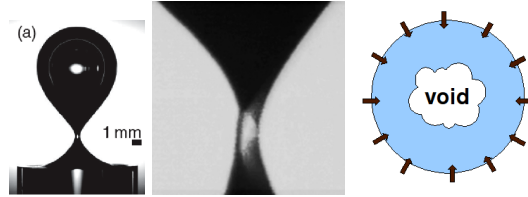


FIG. 1: Bubble disconnection dynamics. (a) Experimental setup: an air bubble (dark area) is submerged under water and released from a nozzle which has been tilted by 2° from the horizontal. Bright spots are optical artifacts. (b) Snap shot of the bubble neck near disconnection. White area indicate water. Photos courtesy of Keim & Nagel [10]. (c) Model: the time-evolution of a cross-section of the bubble neck is modelled as a 2D collapse driven by a radially-symmetric inflow from the far-field.

tion employed by Schmidt et al [9]. Since the vibrations excited by the initial asymmetry retain the same amplitudes while the average radius of the bubble neck decreases towards 0, the bubble neck always becomes severely distorted. We simulate the interface evolution in this strong distortion regime. We find that, when an initial asymmetry is present, the axisymmetric implosion is never attained. Instead the interface often evolves into a smooth self-contact. The bubble interface intersects itself and creates several vertical lobes, in qualitative agreement with the experiment (Fig. 1b). We show this smooth contact evolves naturally from a single vibration persisting until the void shape becomes multiply connected. As a result an intricate memory of the initial distortion is retained until contact.

Our model follows the approach outlined in [2]. We assume that the bubble neck is strongly elongated along the vertical direction. In this long-wavelength limit, the leading-order evolution of the air-water interface is two-dimensional (2D): every cross-section of the bubble neck contracts solely due to the influx of water in the same horizontal plane, with no influence from the dynamics at other heights. The disconnection thus reduces to a 2D version of the classic Rayleigh-Plesset collapse [14].

We also neglect the effects of air flow within the bubble neck and surface tension at the interface. Both effects can modify but do not change the essential features of our results. Despite these simplifications, the 2D model is surprisingly accurate, quantitatively reproducing the measured inertial implosion dynamics until the bubble neck is a few microns across [9].

Fig. 1c illustrates the 2D model. A distorted void, modelled as a region of constant and uniform pressure, is immersed in water. Far from the void, we impose a radially symmetric inflow. To simplify the arithmetic, we choose the reference pressure level such that the void pressure is exactly at $p = 0$. We also require that the 2D volume flux of the far-field flow remain constant over time. This forcing condition produces an average implosion dynamics consistent with the leading-order behavior of the measured disconnection [3, 6, 7, 8, 9, 10]. We use a polar coordinate system whose origin coincides with the center of the void. The air-water interface is given by $r = S(\theta, t)$. Since viscous effects are negligible, the exterior velocity field is irrotational, i.e. $\mathbf{u}(\mathbf{x}, t) = \nabla\Phi$ where Φ is a velocity potential. Since the exterior flow is also incompressible $\nabla \cdot \mathbf{u} = 0$, the velocity potential Φ satisfies Laplace's equation $\nabla^2\Phi = 0$. Far from the void surface, the exterior flow approaches the form, $(-Q/r)\mathbf{e}_r$, where $2\pi Q$ is the volume flux. Two boundary conditions dictate the time-evolution of the velocity potential $\Phi(r, \theta, t)$ and the interface $S(\theta, t)$. First, at the rapidly accelerating void surface, the normal stress exerted by the exterior flow must equal the void pressure. This unsteady version of the Bernoulli condition has the form

$$[\partial\Phi/\partial t + (1/2)|\nabla\Phi|^2]|_S = 0. \quad (1)$$

Second, the position \mathbf{x} of a material point on the surface is advected by the exterior flow,

$$\frac{d\mathbf{x}}{dt} = \left(\frac{\partial}{\partial t} + \nabla\Phi \cdot \nabla \right) \mathbf{x} = \nabla\Phi|_S \quad (2)$$

To solve for the time evolution, we use an approach developed by Dyachenko et al. [15, 16], which has two key steps. First, the solution of $\nabla^2\Phi = 0$ in the exterior is simplified by mapping the exterior of the 2D interface $S(\theta, t)$ conformally onto the exterior of a unit circle in the complex plane w [17]. A point on the w -plane is related to the location (r, θ) on the 2D plane by $z(w, t) = re^{i\theta}$. The velocity potential in the physical plane is then given by the real part of a complex velocity potential Ψ . This simplification is obtained at the cost of transforming the governing equations for the time evolution, (1) and (2), into more complicated forms. The second step ameliorates this defect. Rather than solving directly for the interface $z = S(\theta, t)e^{i\theta}$ and the complex potential Ψ , we work with

$$\mathcal{R}(w, t) = 1/(w\partial_w z) \quad \mathcal{V}(w, t) = (\partial_w \Psi)/(\partial_w z). \quad (3)$$

The variable \mathcal{V} corresponds to the speed of the fluid motion on the interface. The variable \mathcal{R} does not have a

straight forward physical interpretation, though it clearly is a measure of how distorted the void shape in the real space has become relative to the unit circle on the w -plane. The evolution equations (1) and (2) now assume the form

$$\partial_t \mathcal{R} = w \mathcal{R}' \mathcal{A} \{ \text{Re}[\mathcal{R}\mathcal{V}^*] \} - w \mathcal{R} \mathcal{A}' \{ \text{Re}[\mathcal{R}\mathcal{V}^*] \} \quad (4)$$

$$\partial_t \mathcal{V} = w \mathcal{V}' \mathcal{A} \{ \text{Re}[\mathcal{R}\mathcal{V}^*] \} - w \mathcal{R} \mathcal{A}' \{ |\mathcal{V}|^2 \} / 2 \quad (5)$$

where the prime index denotes the derivative with respect to w and $*$ corresponds to complex conjugate. The integral operator \mathcal{A} is given by the Cauchy integral [17, 18]: To solve for the void evolution, we expand \mathcal{R} and \mathcal{V} as $\mathcal{R} = \sum_{n=0}^N c_n/w^{n+1}$ and $\mathcal{V} = \sum_{n=0}^N d_n/w^{n+1}$ where N is the total number of terms in the expansion and the coefficients c_n and d_n are computed from Ψ and S . This reformulation speeds up the numerical computation because the right hand side of equations (4,5) can be computed in $N \log N$ steps using the Fast Fourier Transform. We have implemented a version of the numerical solution described above using *Mathematica* and obtained results with a total of 256 terms in the expansion (6). We have also checked that results which involve more distorted final shapes are robust by implementing a version of the code in C++ and solving it with $N = 1024$.

A typical time evolution is given in Fig. 2. At $t = 0$ the void shape is a nearly circular oval given by $S(\theta, t = 0) = R_0 + A_2 \cos \Omega_2 \cos(2\theta)$ where R_0 is the initial value of the average radius, A_2 the size of the azimuthal distortion and Ω_2 the initial value for the phase of the standing wave. As time goes on, the void area $\pi \bar{R}^2(t)$ decreases as $\pi R_0^2 - 2\pi Q t$, where $\bar{R}(t)$ is the average radius. To display how the distortion develops, we rescaled the successive shapes by $\bar{R}(t)$. The initial asymmetry excites an $n = 2$ vibration. During the early moments, $A_2 \ll \bar{R}(t)$. In this weak-distortion regime, the numerics agree quantitatively with the linear stability results by Schmidt et al. [9]. The distorted void vibrates as

$$\begin{aligned} S(\theta, t) &= \bar{R}(t) + A_2 \cos[\phi_2(\bar{R})] \cos(2\theta) \\ \phi_2(\bar{R}) &= \ln(R_0/\bar{R}(t)) + \Omega_2. \end{aligned} \quad (6)$$

Over time, the amplitude of the vibration A_2 remains constant while the phase of the vibration ϕ_2 oscillates. In \mathcal{R} and \mathcal{V} , the vibration described by the eqn. (6) has the form

$$\begin{aligned} \mathcal{R}(w, t) &= \frac{1}{w\bar{R}(t)} \left[1 + \left(\frac{A_2}{R_0} \right) \frac{\cos \phi_2}{w^2 \bar{R}(t)} \right] \\ \mathcal{V}(w, t) &= \frac{1}{w\bar{R}(t)} \left[-1 + \left(\frac{A_2}{R_0} \right) \frac{\sin \phi_2}{w^2 \bar{R}(t)} \right] \end{aligned} \quad (7)$$

which is simply a truncated series containing only the first 2 terms in the expansion for \mathcal{R} and \mathcal{V} . In Fig. 2 the standing wave excited by the initial asymmetry is evident in the first 3 images. The void is initially elongated along the x -axis, then becomes elongated along the y -axis ($\bar{R}/R_0 = 0.04$) and later is elongated along the x -axis ($\bar{R}/R_0 = 0.02$). In the strong distortion regime

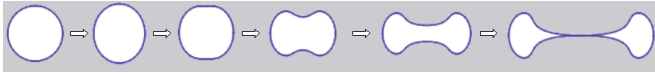


FIG. 2: Time-evolution of an initially elongated void ($A_2/R_0 = 0.004$, $\Omega_2 = -\pi/4$). The successive shapes are rescaled by the average radius \bar{R} . From left to right, the shapes are taken at $\bar{R}/R_0 = 1, 0.04, 0.02, 0.01, 0.005$ and 0.0023127 .

($A_2 \approx \bar{R}(t)$), the inward-curving portions of the interface protrude further and broaden. Finally the void surface collides with itself. The interface shape at contact remains smooth. In contrast, eqn. (6), derived assuming that the distortion is weak, predicts a curvature singularity at contact, corresponding to the opposite sides of the surface meeting in a wedge.

The rest of the paper focuses on this smooth contact. Simulations with many different initial shapes show this to be the most common outcome. The implosion into a point predicted by the axisymmetric model is never attained when an initial asymmetry is present. Other outcomes are possible. Occasionally, the inward-curving portion of the interface can broaden so rapidly that it splits into two minima before the void surface manages to collide with itself. Long and narrow "fingers" of water intruding into the void are also seen, though numerical instabilities prevent us from following the evolution until the first shape transition.

One interpretation of the wedge singularity in eqn. (6) being replaced by smooth contact in the full simulation is that the interactions between different vibrations regularize the time evolution, thus smoothing out the curvature singularity. Below we show that there is a simpler way to think about the result. While some smoothing of the collision does take place, the non-singular contact in fact evolves from the persistence of a single vibration. To see this, note that when the void shape is strongly distorted from a circle, the form of the standing wave on the void surface distorts from $\cos(n\theta)$. This distortion is naturally captured by the $\mathcal{R}(w, t)$ and $\mathcal{V}(w, t)$ variables, since their evolution, involving only solving Laplace's equation in the exterior of a unit circle and eqns. (4,5), are considerably simpler than those for Φ and S . To demonstrate this, in Fig. 3 we plot the time evolution of a hypothetical interface $S(\theta, t)$ governed by the truncated expansion (7). The initial shape is identical with the initial asymmetry used to start the full simulation in Fig. 2. From left to right, the average radius $\bar{R}(t)$ decreases while the vibration persists (A_2 remains fixed). When $A_2 \ll \bar{R}(t)$ (first 3 images in Fig. 3), eqn (7) describes the same shape vibration as eqn. (6). When $\bar{R}(t) \approx A_2$, however, the conformal mapping transforming the expansion in the mathematical plane to the void shape in physical space is considerably different, primarily because the transformation involves $\partial_w z$. When the truncated expansion (7) is extrapolated down to the first shape transition, the evolution reproduces all the qualitative features from the

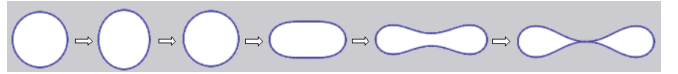


FIG. 3: Time-evolution according to truncated series (7). ($A_2/R_0 = 0.004$, $\Omega_2 = -\pi/4$). The successive shapes are rescaled by the average radius \bar{R} . From left to right, $\bar{R}/R_0 = 1, 0.04, 0.02, 0.01, 0.005$ and 0.0035594 .

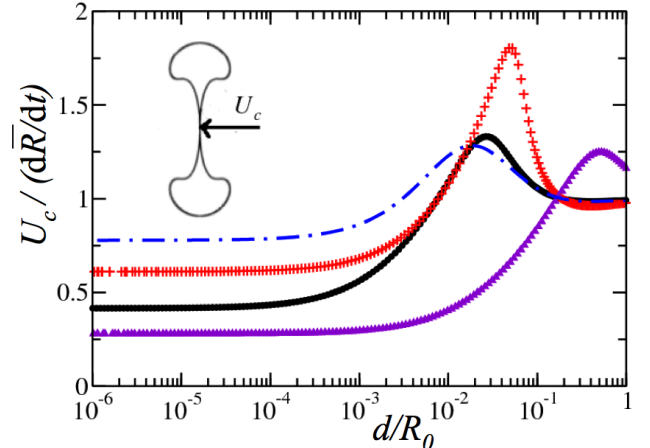


FIG. 4: Rescaled velocity at the contact location $U_c / (d\bar{R}/dt)$ as a function of the gap width d/R_0 . The dot-dash line plots curve due to the truncated series (7) and initial conditions $A_2/R_0 = 0.004, \Omega_2 = -\pi/4$. The solid circles are results from the simulation for the same initial condition. Simulation results for $A_2/R_0 = 0.011$ (crosses) and $A_2/R_0 = 0.067$ (triangles) with the same Ω_2 display the same qualitative behavior but terminate with different U_c values.

full simulation. This shows clearly that a smooth contact, instead of a wedge singularity, evolves from a vibration of constant amplitude imposed over a shrinking void.

This idea that contact evolves from the persistence of single vibrational mode also allows us to quantitatively estimate how the contact forms. Fig. 4 plots $U_c / (d\bar{R}(t)/dt)$, the rescaled velocity at the contact location, as a function of the dimensionless gap width d/R_0 . Initially the gap distance d is large and the contact location accelerates inwards faster than the void shrinks on average. This acceleration reaches a maximum then decays onto a constant value. The velocity U_c calculated from the truncated series (7) corresponding to a single vibration persisting until contact displays the same behavior. Comparing between the calculation and the full simulation reveals that, initially, the interaction between the $n = 2$ vibration and other vibrational modes present in the full simulation speeds up the contact, shifting the peak in $U_c / (d\bar{R}/dt)$ to a larger value of d . Later, the effect reverses and slows contact. Simulation with different initial distortion amplitudes show the same qualitative evolution. In all the cases examined, the truncated series (7) yields estimates in rough agreement with the numerics.

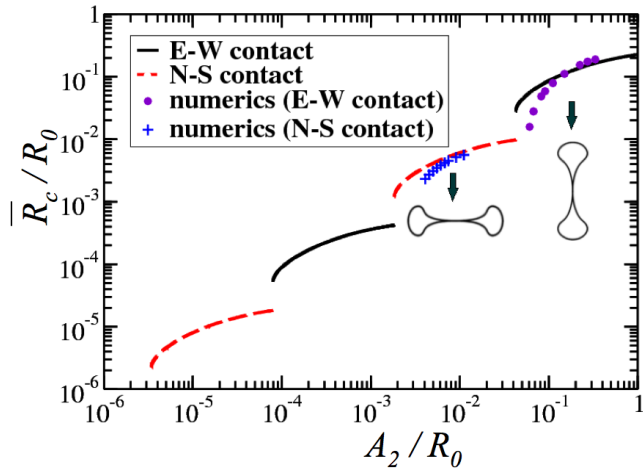


FIG. 5: The dimensionless average radius \bar{R}_c/R_0 at the moment of contact as a function of the initial distortion amplitude A_2/R_0 . The gap in the numerical result corresponds to initial conditions that evolve into fingers of water.

Finally we show that eqn. (7) provides a simple and roughly correct estimate for \bar{R}_c , the average radius of the void at first contact. This is the characteristic length-scale below which the initial asymmetry causes the interface evolution to deviate significantly from an axisymmetric implosion and the energy focusing is cut-off. Fig. 5 plots \bar{R}_c as a function of the initial asymmetry A_2/R_0 . Since a smaller initial asymmetry allows the leading-order, axisymmetric implosion to proceed further, \bar{R}_c decreases with A_2 . What is striking is that the decrease does not proceed at a uniform rate but instead has an intricate structure. This is because the contact evolves from a vibration which oscillates over time, so that the narrowest "waist" of the void can be oriented either along the x -axis (east-west orientation) or along the y -axis (north-south orientation). The abrupt jumps between the different branches of the analytic result correspond to this change in the orientation. Reducing A_2 causes the contact orientation to transform successively, first from an east-west one into a north-south one, then back into an east-west orientation and so on and so forth. We observe the same pattern of switching orientation in the numerics. Within each branch, \bar{R}_c initially changes

slowly, and then more rapidly, as A_2 is reduced. This reflects the fact that a contact formed when the vibration is "in-sync", i.e. at its maximum shape distortion, requires a smaller initial distortion amplitude than a contact formed when the vibration is slightly out of sync.

We emphasize that the collision of the void surface with itself is neither a physical singularity, one corresponding to a divergence in the velocity or the pressure, nor a mathematical singularity. This makes the collision process different from both the cusp-formation process analyzed by Shraiman & Bensimon [17, 19] as well as the bubble break-up dynamics analyzed by [20]. These shape evolutions in a Hele-Shaw cell terminate when one or more singularities of the mapping function cross the unit circle representing the interface on the complex plane. Here the mapping remains perfectly smooth. Mathematically, the contact analyzed here does not correspond to an evolution towards an isolated attractor in the phase space spanned by the trajectories of solutions for S and Φ . Instead, the bubble disconnection problem is associated with a phase space which has a natural boundary, a "wall" separating singly-connected void shapes from the multiply-connected ones. A self-contact corresponds to a time evolution that intersects a point on the "wall" in a finite amount of time. This is why the dynamics near contact is not universal but instead retains an intricate memory of the initial distortion.

In conclusion, we have conducted a numerical study of asymmetric bubble disconnection. The simulations show that an initial distortion excites vibrations which persist until the interface collides with itself. This idea also provides a simple way to calculate both how a contact forms over time and \bar{R}_c , the critical length below which energy focusing is cut-off by the slight initial asymmetry. The results of this simple estimate capture all the qualitative trends and are in rough agreement with results from a full numerical simulation.

We thank I. Gruzberg, N. C. Keim, D. Lohse, S. R. Nagel, L. E. Schmidt and P. Wiegmann for encouragement and feedback. This work was supported by NSF-MRSEC No. DMR-0820054 (K.S.T.) and NSF No. CBET 0730629 (W.W.Z)

[1] G. Birkhoff and E. H. Zarantonello, *Jets, wakes and cavities* (Academic Press, New York, 1957).

[2] M. S. Longuet-Higgins, B. R. Kerman, and K. Lunde, *J. Fluid Mech.* **230**, 365 (1991).

[3] J. C. Burton, R. Waldrep, and P. Taborek, *Phys. Rev. Lett.* **94**, 184502 (2005).

[4] H. N. Oguz and A. Prosperetti, *J. Fluid Mech.* **257**, 111 (1993).

[5] J. M. Gordillo, A. Sevilla, J. Rodríguez-Rodríguez, and C. Martínez-Bazán, *Phys. Rev. Lett.* **95**, 194501 (2005).

[6] R. Bergmann, D. van der Meer, M. Stijnman, M. Sandtke, A. Prosperetti, and D. Lohse, *Phys. Rev. Lett.* **96**, 154505 (2006).

[7] S. T. Thoroddsen, T. G. Etoh, and K. Takehara, *Phys. Fluids* **19**, 042101 (2007).

[8] J. Eggers, M. A. Fontelos, D. Leppinen, and J. H. Snoeijer, *Phys. Rev. Lett.* **98**, 094502 (2007).

[9] L. E. Schmidt, N. C. Keim, W. W. Zhang, and S. R. Nagel, *Nature Phys.* (2008), accepted.

[10] N. C. Keim, P. Moller, W. W. Zhang, and S. R. Nagel,

Phys. Rev. Lett. **97**, 145503 (2006).

[11] P. Doshi, I. Cohen, W. W. Zhang, M. Siegel, P. Howell, O. A. Basaran, and S. R. Nagel, Science **302**, 1185 (2003).

[12] X. D. Shi, M. P. Brenner, and S. R. Nagel, Science **265**, 219 (1994).

[13] J. Eggers, Rev. Mod. Phys. **69**, 865 (1997).

[14] L. D. Landau and E. M. Lifshitz, *Fluid Mechanics* (Butterworth-Heinemann, Oxford, 1987).

[15] A. I. Dyachenko, E. A. Kuznetsov, M. D. Spector, and V. E. Zakharov, Phys. Lett. A **221**, 73 (1996).

[16] V. E. Zakharov, A. I. Dyachenko, and O. A. Vasilyev, Europ. J. Mech. B **21**, 283 (2002).

[17] B. Shraiman and D. Bensimon, Phys. Rev. A **30**, 2840 (1984).

[18] G. F. Carrier, M. Krook, and C. E. Pearson, *Functions of a complex variable* (McGraw-Hill, New York, 1966).

[19] S. Tanveer, J. Fluid Mech. **409**, 273 (2000).

[20] S. Y. Lee, E. Bettelheim, and P. Wiegmann, Physica D **219**, 22 (2006).